Subproblem h-Conform Magnetodynamic Finite Element Formulation for Accurate Model of Multiply Connected Thin Regions

Vuong Q. Dang[1,a], Patrick Dular[1,2], Ruth V. Sabariego[1], Laurent Krähenbühl[3] and Christophe Geuzaine[1]

[1]University of Liège, Dept. of Electrical Engineering and Computer Science, ACE, B-4000 Liège, Belgium
[2]Fonds de la Recherche Scientifique - F.R.S.-FNRS, B-1000 Brussels, Belgium
[3]University of Lyon, Ampère (CNRS UMR5005), École Centrale de Lyon, F-69134 Écully Cedex, France

Abstract. A subproblem h-conform eddy current finite element method is proposed for correcting the inaccuracies inherent to thin shell models. Such models replace volume thin regions by surfaces but neglect border effects in the vicinity of their edges and corners. The developed surface-to-volume correction problem is defined as a step of the multiple subproblems applied to a complete problem, consisting of inductors and magnetic or conducting regions, some of these being thin regions. The general case of multiply connected thin regions is considered.

1 Introduction

Thin shell (TS) finite element (FE) models [1], [2], [5], assume that the fields in the thin regions are approximated by a *priori* 1-D analytical distributions along the shell thickness. In the frame of the FE method, their interior is thus not meshed and is rather extracted from the studied domain, being reduced to a zero-thickness double layer with interface conditions (ICs) linked to the inner analytical distributions. This means that corner and edge effects are neglected.

To overcome these drawbacks, the subproblem method (SPM) for the h-conform FE formulation has been already developed in [3] for simply connected TS regions, proposing a surface-to-volume local correction. The method is herein extended to multiply connected TS regions, i.e. regions with holes, for both the associated surface model (alternative to the method in [5], [6]) and its volume correction. The global currents flowing around the holes and their associated voltages are naturally coupled to the local quatities, via some cuts for magnetic scalar potential discontinuities at both TS and correction steps.

A reduced model (SP q) with the inductors alone is first considered before adding the TS FE (SP p), followed by the volume correction (SP k). From SP q to SP p, the solution q contributes to the surface sources (SSs) for the added TS, with TS ICs [2]. From SP p to SP k, SSs and volume sources (VSs) allow to suppress the TS and cut discontinuities and simultaneously add the actual volume

of the thin region, with its own cut discontinuity. Each SP requires a proper adapted mesh of its regions. The method is illustrated and validated on a practical problem.

2 Thin shell correction in the subproblem method

2.1 Canonical magnetodynamic problem

A canonical magnetodynamic problem i, to be solved at step i of the SPM, is defined in a domain Ω_i, with boundary $\partial\Omega_i = \Gamma_i = \Gamma_{h,i} \cup \Gamma_{b,i}$. The eddy current conducting part of Ω_i is denoted $\Omega_{c,i}$ and the non-conducting region $\Omega_{c,i}^C$, with $\Omega_i = \Omega_{c,i} \cup \Omega_{c,i}^C$. Stranded inductors belong to $\Omega_{c,i}^C$, whereas massive inductors belong to $\Omega_{c,i}$. The equations, material relations and boundary conditions (BCs) of the SPs $i = q, p$ and k are

$$\operatorname{curl} \boldsymbol{h}_i = \boldsymbol{j}_i \,, \ \operatorname{div} \boldsymbol{b}_i = 0 \,, \ \operatorname{curl} \boldsymbol{e}_i = -\partial_t \boldsymbol{b}_i \qquad \text{(1a-b-c)}$$

$$\boldsymbol{b}_i = \mu_i \boldsymbol{h}_i + \boldsymbol{b}_{s,i} \,, \ \boldsymbol{e}_i = \sigma_i^{-1} \boldsymbol{j}_i + \boldsymbol{e}_{s,i} \qquad \text{(2a-b)}$$

$$\boldsymbol{n} \times \boldsymbol{h}_i|_{\Gamma_{h,i}} = \boldsymbol{j}_{f,i} \,, \ \boldsymbol{n} \cdot \boldsymbol{b}_i|_{\Gamma_{b,i}} = \boldsymbol{b}_{f,i} \qquad \text{(3a-b)}$$

$$\boldsymbol{n} \times \boldsymbol{e}_i|_{\Gamma_{e,i} \subset \Gamma_{b,i}} = \boldsymbol{k}_{f,i} \qquad \text{(3c)}$$

where $\boldsymbol{h}_i$ is the magnetic field, $\boldsymbol{b}_i$ is the magnetic flux density, $\boldsymbol{e}_i$ is the electric field, $\boldsymbol{j}_i$ is the electric current density, μ_i is the magnetic permeability, σ_i is the electric conductivity and $\boldsymbol{n}$ is the unit normal exterior to Ω_i. In what follows the notation $[\cdot]_{\gamma_i} = |_{\gamma_i^+} - |_{\gamma_i^-}$ expresses the discontinuity of a quantity through an interface γ_i (with

^{a} E-mail: quocvuong.dang@ulg.ac.be

sides γ_i^+ and γ_i^-) in Ω_i, defining ICs. The fields $\boldsymbol{b}_{s,i}$ and $\boldsymbol{e}_{s,i}$ in (2a-b) are VSs that can be used for expressing changes of permeability or conductivity respectively [13].

The fields $\boldsymbol{j}_{f,i}$, $\boldsymbol{b}_{f,i}$ and $\boldsymbol{k}_{f,i}$ in (3a-b-c) are SSs and generally equal zero with classical homogeneous BCs. Their discontinuities via ICs are also equal to zero for common continuous field traces $\boldsymbol{n} \times \boldsymbol{h}_i$, $\boldsymbol{n} \cdot \boldsymbol{b}_i$ and $\boldsymbol{n} \times \boldsymbol{e}_i$. If nonzero, they define possible SSs that account for particular phenomena occuring in the idealized thin region between γ_i^+ and γ_i^- [13]. This is the case when some field traces in SP p are forced to be discontinuous, whereas their continuity must be recovered via a SP k, which is done via a SS in SP k fixing the opposite of the trace discontinuity solution of SP p.
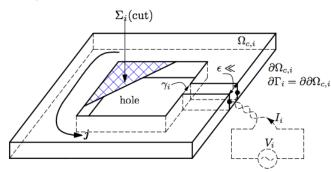

Fig. 1. 3D plate with a source of electromotive force

2.2 From SP q to SP p - inductor alone to TS model

The TS model for the $\boldsymbol{h}_i$-formulation requires an unknown discontinuity $\boldsymbol{h}_{d,i}$ through the TS $\gamma_{t,i}$ of the tangential component $\boldsymbol{h}_{t,i} = (\boldsymbol{n} \times \boldsymbol{h}_i) \times \boldsymbol{n}$ of $\boldsymbol{h}_i$ [2], i.e.

$$[\boldsymbol{h}_{t,i}]_{\gamma_{t,i}} = \boldsymbol{h}_{d,i} \ \text{ or } \ [\boldsymbol{n} \times \boldsymbol{h}_i]_{\gamma_{t,i}} = \boldsymbol{n} \times \boldsymbol{h}_{d,i} \quad (4)$$

with $\boldsymbol{h}_{d,i}$ fixed to zero along the TS border to prevent any current to flow through it. In order to explicitly express the discontinuity, field $\boldsymbol{h}_i$ is written on both sides of $\gamma_{t,i}$ as

$$\boldsymbol{h}_i|_{\gamma_{t,i}^+} = \boldsymbol{h}_{c,i} + \boldsymbol{h}_{d,i} \,, \ \boldsymbol{h}_i|_{\gamma_{t,i}^-} = \boldsymbol{h}_{c,i} \quad (5)$$

with $\boldsymbol{h}_{c,i}$ its continuous component; (5) can be also applied to the tangential components $\boldsymbol{h}_{t,i}$, $\boldsymbol{h}_{t,c,i}$ and $\boldsymbol{h}_{t,d,i}$.

SSs for SP p are to be defined via BCs and ICs of impedance-type BCs (IBC) given by the TS model [2] combined with contributions from SP q. There is no thin region in SP q, but in order to get a relative constraint between SP q and SP p via the corresponding ICs with $\gamma_t = \gamma_t^\pm = \gamma_q^\pm = \gamma_p^\pm = \Gamma_{ts,q}^\pm = \Gamma_{ts,p}^\pm$ and $\boldsymbol{n}_t = -\boldsymbol{n}$ for the TS, one has to imagine that a thin region appears in SP q. One gets for SP q and SP p [2], [3]

$$[\boldsymbol{n} \times \boldsymbol{e}_q]_{\gamma_q} = \boldsymbol{n} \times \boldsymbol{e}_q|_{\gamma_q^+} - \boldsymbol{n} \times \boldsymbol{e}_q|_{\gamma_q^-} = 0 \quad (6)$$

$$[\boldsymbol{n} \times \boldsymbol{e}]_{\gamma_p} = [\boldsymbol{n} \times \boldsymbol{e}_q]_{\gamma_p} + [\boldsymbol{n} \times \boldsymbol{e}_p]_{\gamma_p} = \mu\beta \, \partial_t(2\boldsymbol{h}_c + \boldsymbol{h}_d) \quad (7)$$

$$\boldsymbol{n} \times \boldsymbol{e}_p|_{\gamma_p^+} = \frac{1}{2}\Big[\mu\beta \, \partial_t(2\boldsymbol{h}_c + \boldsymbol{h}_d) + \frac{1}{\sigma\beta}\,\boldsymbol{h}_d\Big] - \boldsymbol{n} \times \boldsymbol{e}_q|_{\gamma_p^+} \quad (8)$$

$$\beta = \gamma_i^{-1} \tanh(\frac{d_i \gamma_i}{2}), \gamma_i = \frac{1+j}{\delta_i}, \delta_i = \sqrt{\frac{2}{\omega\sigma_i\mu_i}} \quad (9)$$

where d_i is the local TS thickness, δ_i is the skin depth in the TS, $\omega = 2\pi f$, f is the frequency, j is the imaginary unit and $\partial_t \equiv j\omega$. The discontinuity $[\boldsymbol{n} \times \boldsymbol{e}_q]_{\gamma_p}$ in (7) does not need any correction because solution SP q presents no such discontinuitiy, i.e. $[\boldsymbol{n} \times \boldsymbol{e}_q]_{\gamma_q} = [\boldsymbol{n} \times \boldsymbol{e}_q]_{\gamma_p} = 0$.

2.3 From SP p to SP k - TS to volume model

The obtained TS solution in SP p is then corrected by SP k that overcomes the TS assumptions [2]. The SPM offers the tools to implement such as refinement, thanks to simultaneous SSs and VSs. A fine volume mesh of the shell is now required and is extended to its neighborhood without including the other regions of previous SPs. This allows to focus on the fineness of the mesh only in the shell. SP k has to suppress the TS representation via SSs opposed to TS ICs, in parallel to VSs in the added volume shell [3] that accounts for volume change of μ_p and σ_p in SP p to μ_k and σ_k in SP k (with $\mu_p = \mu_0$, $\mu_k = \mu_{r,volume}$, $\sigma_p = 0$ and $\sigma_k = \sigma_{volume}$). This correction is usually limited to the neighborhood of the shell, which permits to benefit from a reduction of the extension of the associated mesh [3]. The VSs for SP k are [3], [12], [13]

$$\boldsymbol{b}_{s,k} = (\mu_k - \mu_p)(\boldsymbol{h}_q + \boldsymbol{h}_p) \quad (10)$$

$$\boldsymbol{e}_{s,k} = -(\boldsymbol{e}_q + \boldsymbol{e}_p) \quad (11)$$

3 Finite element weak formulations
3.1 h-ϕ formulation with source and reaction magnetic fields

The weak $\boldsymbol{h}_i$-ϕ_i formulation is obtained from the weak form of Faraday's law (1c) [13]. The magnetic field $\boldsymbol{h}_i$ is split into two parts, i.e.

$$\boldsymbol{h}_i = \boldsymbol{h}_{s,i} + \boldsymbol{h}_{r,i} \quad (12)$$

where $\boldsymbol{h}_{s,i}$ is a source magnetic field due to the fixed current density $\boldsymbol{j}_{s,i}$ such that $\operatorname{curl} \boldsymbol{h}_{s,i} = \boldsymbol{j}_{s,i}$, and $\boldsymbol{h}_{r,i}$ is the reaction magnetic field. In non-conducting regions $\Omega_{c,i}^C$, field $\boldsymbol{h}_{r,i}$ is defined via a scalar potential ϕ_i, i.e. $\boldsymbol{h}_{r,i} = -\operatorname{grad}\phi_i$. Potential ϕ_i in a multiply connected $\Omega_{c,i}^C$ is multivalued (Fig. 1) and is made singlevalued via the definition of cuts through each hole of $\Omega_{c,i}$ [7], [9]. The constraints associated with the cut and the discontinuity of the tangential component of the magnetic field across the thin structures are expressed in Section 3.2. The weak forms for SP q and SP p are

$$\partial_t(\mu_q\boldsymbol{h}_q, \boldsymbol{h}_q')_{\Omega_q} + \partial_t(\mu_q\boldsymbol{h}_{s,q}, \boldsymbol{h}_q')_{\Omega_q} + \langle\boldsymbol{n} \times \boldsymbol{e}_q, \boldsymbol{h}_q'\rangle_{\Gamma_{e,q}} +$$
$$\langle[\boldsymbol{n} \times \boldsymbol{e}_q]_{\gamma_q}, \boldsymbol{h}_q'\rangle_{\gamma_q} = 0 \,, \ \forall\boldsymbol{h}_q' \in F_{q,h\phi}^1(\Omega_q) \quad (13)$$

$$\partial_t(\mu_p\boldsymbol{h}_p, \boldsymbol{h}_p')_{\Omega_p} + \langle\boldsymbol{n} \times \boldsymbol{e}_p, \boldsymbol{h}_p'\rangle_{\Gamma_{e,p}}$$
$$+\langle[\boldsymbol{n} \times \boldsymbol{e}_p]_{\gamma_p}, \boldsymbol{h}_p'\rangle_{\gamma_p} = 0 \,, \ \forall\boldsymbol{h}_p' \in F_{p,h\phi}^1(\Omega_p) \quad (14)$$

where $F_{i,h\phi}^1(\Omega_i)$ in (13) and (14) is a curl-conform function space (built with edge FEs at the discrete level) defined

on Ω_i and containing the basis functions for $\boldsymbol{h}_i$ (coupled to ϕ_i) as well as for the test function $\boldsymbol{h}'_i$; $(\cdot,\cdot)_{\Omega_i}$ and $<\cdot,\cdot>_{\Gamma_i}$ respectively, denote a volume intergal in Ω_i and a surface intergal on Γ_i of the product of their vector field arguments. The surface integral term on $\Gamma_{e,i}$ accounts for natural BCs of type (3c), usually zero.

The term $\langle[\boldsymbol{n}\times\boldsymbol{e}_p]_{\gamma_p},\boldsymbol{h}'_p\rangle_{\gamma_p}$ in (14) is used to weakly express the electric field TS IC proper to the TS model [2], i.e

$$\langle[\boldsymbol{n}\times\boldsymbol{e}_p]_{\gamma_p},\boldsymbol{h}'_p\rangle_{\gamma_p} = \langle[\boldsymbol{n}\times\boldsymbol{e}_p]_{\gamma_p},\boldsymbol{h}'_c+\boldsymbol{h}'_d\rangle_{\gamma_p}$$
$$= \langle[\boldsymbol{n}\times\boldsymbol{e}_p]_{\gamma_p},\boldsymbol{h}'_c\rangle_{\gamma_p} + \langle[\boldsymbol{n}\times\boldsymbol{e}_p]_{\gamma_p},\boldsymbol{h}'_d\rangle_{\gamma_p}. \quad (15)$$

Splitting test function $\boldsymbol{h}'_p$ into continous and discontinuous parts, i.e. $\boldsymbol{h}'_c$ and $\boldsymbol{h}'_d$, with $\boldsymbol{h}'_d$ null on the negative side of TS γ_p^-, like in (5), equation (15) becomes [2]

$$\langle[\boldsymbol{n}\times\boldsymbol{e}_p]_{\gamma_p},\boldsymbol{h}'_p\rangle_{\gamma_p} = \langle[\boldsymbol{n}\times\boldsymbol{e}_p]_{\gamma_p},\boldsymbol{h}'_c\rangle_{\gamma_p}+$$
$$\langle\boldsymbol{n}\times\boldsymbol{e}_p|_{\gamma_{p+}},\boldsymbol{h}'_d\rangle_{\gamma_{p+}}. \quad (16)$$

The trace discontinuity term $\langle[\boldsymbol{n}\times\boldsymbol{e}_p]_{\gamma_p},\boldsymbol{h}'_c\rangle_{\gamma_p}$ in (16) is given by (7), i.e.

$$\langle[\boldsymbol{n}\times\boldsymbol{e}_p]_{\gamma_p},\boldsymbol{h}'_c\rangle_{\gamma_p} = \langle[\boldsymbol{n}\times\boldsymbol{e}]_{\gamma_p},\boldsymbol{h}'_c\rangle_{\gamma_p}$$
$$= \langle\mu\beta\,\partial_t(2\boldsymbol{h}_c+\boldsymbol{h}_d),\boldsymbol{h}'_c\rangle_{\gamma_p}. \quad (17)$$

The term $\langle\boldsymbol{n}\times\boldsymbol{e}_p|_{\gamma_{p+}},\boldsymbol{h}'_d\rangle_{\gamma_{p+}}$ in (16) is given by (8), suppressing $\boldsymbol{n}\times\boldsymbol{e}_q|_{\gamma_{p+}}$ of SP q and simultaneously adding the actual TS BC. Therefore, the term $\langle\boldsymbol{n}\times\boldsymbol{e}_p|_{\gamma_{p+}},\boldsymbol{h}'_d\rangle_{\gamma_{p+}}$ is a SS that is naturally expressed via the weak formulation of SP q (13), i.e.

$$-\langle\boldsymbol{n}\times\boldsymbol{e}_q|_{\gamma_p^+},\boldsymbol{h}'_d\rangle_{\gamma_p^+} = (\mu_q\partial_t\boldsymbol{h}_{s,q},\boldsymbol{h}'_d)_{\Omega_q} + (\mu_q\partial_t\boldsymbol{h}_q,\boldsymbol{h}'_d)_{\Omega_q}. \quad (18)$$

The volume integrals in (18) are also limited to a single layer of FEs touching $\gamma_p^+ = \gamma_q^+ = \Gamma_{ts}^+$, because they involve only the trace $\boldsymbol{n}\times\boldsymbol{h}'_d|_{\gamma_p^+}$. At the discrete level, the source $\boldsymbol{h}_q$, initially in the mesh of SP q, has to be projected in the mesh of SP p via a projectiong method [3], [13]. Then the actual volume SP k corrects the inaccurate TS SP p solution via VSs (10) and (11).

In addition, the surface integral $\langle\boldsymbol{n}\times\boldsymbol{e}_p,\boldsymbol{h}'_p\rangle_{\Gamma_{e,p}}$ in (14) can be extended to a global condition defining a voltage V_i [4], with $\boldsymbol{h}'_p = \boldsymbol{c}_i = -\mathrm{grad}\,q_i$ in $\Omega_{c,p}^C$ with $\boldsymbol{n}\times\boldsymbol{c}_i = -\boldsymbol{n}\times\mathrm{grad}\,q_i$ on $\partial\Omega_{c,p}$ ($\boldsymbol{c}_i$ is the current basis function) made simply connected by cut Σ_i (Figs. 1 and 2). Potential q_i is fixed to 1 on one side of the cut and to 0 on the other side. The continuous transition of q_i between both these value can be implemented in a transition layer in $\Omega_{c,p}^C$ adjacent to side '+' (Figs. 1 and 2), which reduces the suport of q_i and $\boldsymbol{c}_i$. One gets [4]

$$\langle\boldsymbol{n}\times\boldsymbol{e}_p,\boldsymbol{c}_i\rangle_{\partial\Omega_{c,p}} = \oint_{\partial\Gamma_i} q_i\boldsymbol{e}_p.dl = \int_{g_i}\boldsymbol{e}_p.dl = V_i \quad (19)$$

where g_i is a path connecting two real or imaginary electrodes of the thin region.

The weak form of SP k is

$$\partial_t(\mu_k\boldsymbol{h}_k,\boldsymbol{h}'_k)_{\Omega_k} + (\sigma_k^{-1}\mathrm{curl}\,\boldsymbol{h}_k,\mathrm{curl}\,\boldsymbol{h}'_k)_{\Omega_{c,k}} + \partial_t(\boldsymbol{b}_{s,k},\boldsymbol{h}'_k)_{\Omega_k}$$
$$+(\boldsymbol{e}_{s,k},\mathrm{curl}\,\boldsymbol{h}'_k)_{\Omega_k} + \langle[\boldsymbol{n}\times\boldsymbol{e}_k]_{\gamma_k},\boldsymbol{h}'_k\rangle_{\gamma_k} + \langle\boldsymbol{n}\times\boldsymbol{e}_k,\boldsymbol{h}'_k\rangle_{\Gamma_{e,k}}$$
$$= 0,\forall\boldsymbol{h}'_k\in F_{k,h\phi}^1(\Omega_k). \quad (20)$$

3.2 Field discontinuities for multiply connected TS regions

With the TS model, a volume shell initially in $\Omega_{c,i}$ is extracted from Ω_i and then considered with the double layer TS surface $\Gamma_{ts,i}$ [2]. In addition to the electric field IC weakly defined in (14), the TS model requires a magnetic field discontinuity $[\boldsymbol{h}_i]_{\Gamma_{ts,i}} = \boldsymbol{h}_{d,i}$ strongly defined in $F_{i,h\phi}^1(\Omega_i)$ via an IC on both sides of the TS via (5). This can be formulated via a TS discontinuity of ϕ_i, i.e. $[\phi_i]_{\Gamma_{ts,i}} = \Delta\phi_i|_{\Gamma_{ts,i}} = \phi_{d,i}|_{\Gamma_{ts,i}}$ (Fig. 2), with $\phi_i|_{\Gamma_{ts,i}^+} = \phi_{c,i}|_{\Gamma_{ts,i}} + \phi_{d,i}|_{\Gamma_{ts,i}}$ and $\phi_i|_{\Gamma_{ts,i}^-} = \phi_{c,i}|_{\Gamma_{ts,i}}$. The discontinuity $\phi_{d,i}$ is constant on each cut and can be written as

$$\phi_i = \phi_{c,i} + \phi_{d,i}\,(\phi_{d,i} = \Delta\phi_d|_{\Gamma_{cut,i}} = [\phi_{d,i}]_{cut,i}) \quad (21)$$
$$[\phi_i]_{cut,i} = \phi_i|_{\Gamma_{cut,i}^+} - \phi_i|_{\Gamma_{cut,i}^-} = \phi_{d,i}|_{\Gamma_{cut,i}} = I_i \quad (22)$$

where I_i is the global current flowing around the cut [4]. Discontinuities $\phi_{d,i}|_{\Gamma_{ts,i}}$ and $\phi_{d,i}|_{\Gamma_{cut,i}}$ have to be matched at the TS-cuts intersections.
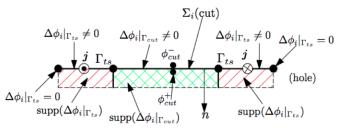

Fig. 2. Section of a 3D plate with a hole, with the associated cut and transition layer (supp) for $\Delta\phi_i$.

3.3 Discretization of the reaction magnetic field

At the discrete level, the use of edge FEs [2], [8] to interpolate curl-conform fields, such as the magnetic filed $\boldsymbol{h}_i$, first gives facilities in defining currents. Indeed, the circulation of such a field along closed path, also being the flux of its curl and consequently the current, is directly obtained from coefficients of the interpolation, in this case those associated with the edges of the path [11].

The magnetic field $\boldsymbol{h}_i$ (12) in formulations (13), (14) and (20) is thus discretized by edge FEs, generating the function space $\in S_i^1(\Omega_i)$ defined on a mesh of Ω_i, i.e.,

$$\boldsymbol{h}_i = \sum_{e\in E(\Omega_i)} h_{e,i}s_{e,i},\quad\forall\boldsymbol{h}_i\in S_i^1(\Omega_i) \quad (23)$$

where $E(\Omega_i)$ is the set of edges of Ω_i, $s_{e,i}$ is the edge basis function associated with edge e and $h_{e,i}$ is the circulation of $\boldsymbol{h}_i$ along the edge e. Now, characterization (23) can be transformed in order to give explicitly the basis functions of the considered discrete space for $F_{h_i,\phi_i}^1(\Omega_i)$ with the essential constraint, i.e., $\boldsymbol{h}_{r,i} = -\mathrm{grad}\,\phi_i$ using the results of [4], [10]. One has

$$\boldsymbol{h}_i = \sum_{e\in E(\Omega_{c,i})-E(\partial\Omega_{c,i})} h_{e,i}s_{e,i} + \sum_{n\in N(\Omega_{c,i}^C)} \phi_{c,n,i}v_{c,n,i}$$
$$+ \sum_{n\in N(\Gamma_{ts,i})} \phi_{d,i}t_{d,n,i} + I_{c_i}\sum_{n\in N(\Gamma_{cut,i})} c_{d,n,i} \quad (24)$$

where $E(\Omega_{c,i}) - E(\partial\Omega_{c,i})$ are the sets of inner edges of the mesh of $\Omega_{c,i}$, without including the edges on its boundary, $N(\Omega_{c,i}^C)$ is the sets of nodes of the mesh of $\Omega_{c,i}^C \cup \partial\Omega_{c,i}^C$, $N(\Gamma_{ts,i})$ is the sets of nodes of the mesh of $\Gamma_{ts,i}$ and $N(\Gamma_{cut,i})$ is the sets of nodes of the mesh of $\Gamma_{cut,i}$ making Ω_c^C simply connected [7]. Coefficients I_{c_i} represent circulations of $\boldsymbol{h}_i$ along well-defined paths given by (22). The functions $t_{d,n,i}$ and $c_{d,n,i}$ can be respectively expressed in the thin regions and the cuts as [2]

$$t_{d,n,i} = \begin{cases} \displaystyle\sum_{\substack{\{n,m\} \in E(\Omega_{c,i}^C) \\ n \in N(\Gamma_{ts,i}) \\ m \notin N(\Gamma_{ts,i}) \\ m \in N_{ts,i}^+}} s_{e,\{n,m\}} \text{ in } \mathrm{supp}(\Delta\phi_i|_{\Gamma_{ts,i}}) \\ \\ \qquad\qquad 0 \qquad\qquad \text{otherwise} \end{cases}$$

$$c_{d,n,i} = \begin{cases} \displaystyle\sum_{\substack{\{n,m\} \in E(\Omega_{c,i}^C) \\ n \in N(\Gamma_{cut,i}) \\ m \notin N(\Gamma_{cut,i}) \\ m \in N_{cut,i}^+}} s_{e,\{n,m\}} \text{ in } \mathrm{supp}(\Delta\phi_i|_{\Gamma_{cut,i}}) \\ \\ \qquad\qquad 0 \qquad\qquad \text{otherwise} \end{cases}$$

where $m \in N_{ts,i}^+$ and $m \in N_{cut,i}^+$ are the sets of nodes of the transition layers $\mathrm{supp}(\Delta\phi_i|_{\Gamma_{ts,i}})$ and $\mathrm{supp}(\Delta\phi_i|_{\Gamma_{cut,i}})$, respectively (Fig. 2).

3.4 TS correction - VSs in the actual volume shell and SSs for suppressing the TS representation

Changes of material properties from μ_p and σ_p in SP p to μ_k and σ_k in SP k, that occur in the volume shell, are taken into account in (20) via the volume integrals $(\boldsymbol{e}_{s,k}, \mathrm{curl}\, \boldsymbol{h}_k')_{\Omega_k}$ and $\partial_t(\boldsymbol{b}_{s,k}, \boldsymbol{h}_k')_{\Omega_k}$. The VS $\boldsymbol{e}_{s,k}$ in (11) is to be obtained from the still undetermined electric fields $\boldsymbol{e}_q$ and $\boldsymbol{e}_p$. Therefore, the field $\boldsymbol{e}_p$ is unknown in any $\Omega_{c,p}^C$. These determinations require to solve an electric problem defined by the Faraday and electric conservation equations [13].

Simultaneously to the VSs in (20), SSs related to ICs [2], [3] compensate the TS and cut discontinuities, i.e, $\phi_{d,p}|_{\Gamma_{ts,p}}$ and $\phi_{d,p}|_{\Gamma_{cut,p}}$, and $[\boldsymbol{n}\times\boldsymbol{e}_p]_{\Gamma_{ts,p}}$ to suppress the TS representation via SSs opposed to ICs, i.e. $\boldsymbol{h}_{d,k} = -\boldsymbol{h}_{d,p}$ and $\phi_{d,k} = -\phi_{d,p}$, and $[\boldsymbol{n}\times\boldsymbol{e}_k]_{\Gamma_{ts,k}} = -[\boldsymbol{n}\times\boldsymbol{e}_p]_{\Gamma_{ts,k}}$. The involed trace $[\boldsymbol{n}\times\boldsymbol{e}_p]_{\Gamma_{ts,k}}$ is naturally expressed via the other integrals in (14), i.e., $\langle[\boldsymbol{n}\times\boldsymbol{e}_k]_{\Gamma_{ts,k}}, \boldsymbol{h}_k'\rangle_{\Gamma_{ts,k}} = -\langle[\boldsymbol{n}\times\boldsymbol{e}_p]_{\Gamma_{ts,k}}, \boldsymbol{h}_k'\rangle_{\Gamma_{ts,k}}$. At the discrete level, this integral is limited to the layer of FEs on both sides $\Gamma_{ts,k}$ of TS, because it involves only the associated trace $\boldsymbol{n}\times\boldsymbol{h}_k'|_{\Gamma_{ts,k}}$. The source $\boldsymbol{h}_p$, with its discontinuity $\boldsymbol{h}_{d,p}$, has also to be transferred from the mesh of TS SP p to the mesh of SP k.

3.5 Projections of solutions between meshes

Some parts of previous solutions serve as sources in a subdomain $\Omega_{s,p} \subset \Omega_p$ of the current SP p, for example from SP q to SP p. At the discrete level, this means that the source quantities $\boldsymbol{h}_q$ have to be expressed in the mesh of SP p, while initially given in the mesh of SP q. This can be done via a projection method [14] of its curl limited to $\Omega_{s,p}$, i.e.

$$(\mathrm{curl}\, \boldsymbol{h}_{q,p-proj}, \mathrm{curl}\, \boldsymbol{h}')_{\Omega_{s,p}} = (\mathrm{curl}\, \boldsymbol{h}_q, \mathrm{curl}\, \boldsymbol{h}')_{\Omega_{s,p}},$$
$$\forall \boldsymbol{h}' \in F_p^1(\Omega_{s,p}) \tag{25}$$

where $F_p^1(\Omega_{s,p})$ is a gauged curl-conform function space for the p-projected source $\boldsymbol{h}_{q,p-proj}$ (the projection of $\boldsymbol{h}_q$ on mesh p) and the test function $\boldsymbol{h}'$. Directly projecting $\boldsymbol{h}_q$ instead of its curl would give numerical inaccuracies when evaluating its curl.

4 Application

The 3D test problem is based on TEAM problem 7: an inductor placed above a thin plate with a hole (Fig. 3) ($\mu_{r,plate} = 1$, $\sigma_{plate} = 35.26$ MS/m). A SP scheme considering three steps is developed. A first FE SP q with the stranded inductor alone is solved on a simplified mesh without any thin regions (Fig. 4, *top*). Then a SP p is solved with the added thin region via a TS FE model (Fig. 4, *middle*). At last, a SP k replaces the TS FEs with the actual volume FEs covering the actual plates with an adequate refine mesh (Fig. 4, *bottom*). The TS error on $\boldsymbol{j}_p$ locally reaches 43% (Fig. 4, *middle*), with plate thickness $d = 19$ mm and frequency $f = 200$ Hz (skin depth $\delta = 6$ mm). The inacuracy on the Joule power loss densities of TS SP p is pointed out by the importance of the correction SP k (Figs. 5 and 6). It reaches several tens of percents along the plate borders and near the plate ends for some critical parameters: e.g., 28% (Fig. 5, *top*) and 32% (Fig. 6, *top*), with $f = 50$ Hz and $\delta = 11.98$ mm in both case, or 53% (Fig. 5, *bottom*) and 61% (Fig. 6, *bottom*), with $f = 200$ Hz and $\delta = 6$ mm in both cases. The errors particularly decrease with a smalller thickness ($d = 2$ mm), being lower than 15% (Fig. 6), with $f = 200$ Hz and $\delta = 6$ mm. Significant errors on the Joule losses and the global currents flowing around the hole for TS SP p are shown in Tables 1 and 2. For $d = 19$ mm and $f = 200$ Hz, the TS error is 13.5% for the global current and 42% for the Joule loss (reduced to 26% for $f = 50$ Hz). For $d = 2$ mm and $f = 200$ Hz, it is respectively reduced to 1% and 6% (4% for $f = 50$ Hz).

5 Conclusions

The SPM allows to accurately correct any TS solution. In particular, accurate corrections of eddy current and power loss densities are obtained at the edges and corners of multiply connected thin regions. All the steps of the method for TS FE have been presented and validated
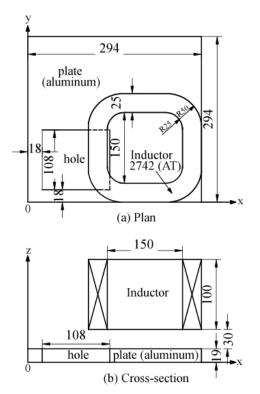
Fig. 3. Geometry of TEAM problem 7: inductor and conducting plate with a hole (all dimensions are in mm).

Table 1. Joule losses in the plate

Thickness d (mm)	Frequency f (Hz)	Thin Shell P_{thin} (W)	Volume P_{vol} (W)	Error (%)
2	50	14.45	13.82	4.36
19	50	5.86	7.95	26.18
2	200	50.44	47.33	6.44
19	200	8.88	15.19	41.51

Table 2. Global currents flowing around the plate hole

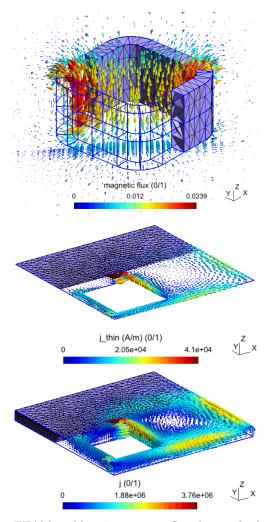| Thickness d (mm)	Frequency f (Hz)	Thin Shell I_{thin} (A)	Volume I_{vol} (A)	Error (%)
2	50	94,5	93.5	1.1
19	50	173.3	199.8	13.2
2	200	190.4	186.5	1.8
19	200	179.3	206.3	14

by coupling SPs via the SPM with the $\boldsymbol{h}$-formulation. Specially, it has been sucessfully applied to the TEAM problem 7.

6 Acknowledgment

References

1. L. Krähenbühl and D. Muller, "Thin layers in electrical engineering. Examples of shell models in analyzing eddy-currents by boundary and finite element methods," IEEE Trans. Magn., vol. 29, no. 2, pp. 1450–1455, 1993.
2. C. Geuzaine, P. Dular, and W. Legros, "Dual formulations for the modeling of thin electromagnetic shells using edge elements," IEEE Trans. Magn., vol. 36, no. 4, pp. 799–802, 2000.
3. Vuong Q. Dang, P. Dular, R. V. Sabariego, L. Krähenbühl and C. Geuzaine, "Subproblem Approach for Thin Shell Dual Finite Element Formulations," IEEE Trans. Magn., vol. 48, no. 2, pp. 407–410, 2012.
4. P. Dular and W. Legros, "Coupling of Local and Global Quantities in Various Finite Element Formulations and its Application to Electrostatics, Magnetostatics and Magnetodynamics," IEEE Trans. Magn., vol. 34, no. 5, pp. 3078–3081, 1998.
5. C. Guérin and G. Meunier, "3-D Magnetic Scalar Potential Finite Element Formulation for Conducting Shells Coupled With an External Circuit," IEEE Trans. Magn., vol. 48, no. 2, pp. 323–326, 2012.
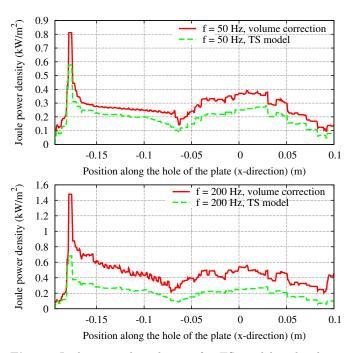6. T. Le-Duc, C. Guérin, O. Chadebec, and J.-M. Guichon "A New Integral Formulation for Eddy Current Computation

Fig. 4. TEAM problem 7: magnetic flux density $\boldsymbol{b}_q$ (in a cut plane) generated by a stranded inductor (*top*), TS eddy current density $\boldsymbol{j}_p$ (*middle*) and its volume correction $\boldsymbol{j}_k$ (*bottom*) (d = 19 mm, f = 200 Hz).

Fig. 5. Joule power loss density for TS model and volume correction along hole and plate borders ($d = 19$ mm).

Fig. 6. Joule power loss density for TS model and volume correction through the hole ($d = 19$ mm).

Fig. 7. Joule power loss density for TS model and volume correction along hole and plate borders (*top*) and through the hole (*bottom*) ($d = 2$ mm).

in Thin Conductive Shells," IEEE Trans. Magn., vol. 48, no. 2, pp. 427–430, 2012.

7. A. Bossavit, "Magnetostatic problems in multiply connected regions: some properties of the curl operator," IEE Proc. vol. 135, no. 3, pp. 179–187, 1988.

8. A. Bossavit, "A rationale for edge-elements in 3D fields computations," IEEE Trans. Magn., vol. 24, no. 1, pp. 74–79, 1988.
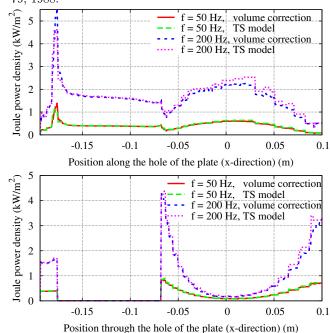
9. D. Rodger and N. Atkinson, "3D eddy currents in multiply connected thin sheet conductors," IEEE Trans. Magn., vol. 23, no. 5, pp. 3047–3049, 1987.

10. P. Dular, J.Y. Hody and A. Nicolet and A.Genon and A. Gennon and W. Legros, "Mixed finite elements associated with a collection of tetrahedra, hexahedra and prism," IEEE Trans. Magn., vol. 30, no. 5, pp. 2980-2983, 1994.

11. P. Dular, F. Henrotte and A. Gennon and W. Legros, "A generlized source magnetic field calculation method for inductors of any shape," IEEE Trans. Magn., vol. 33, no. 2, pp. 1398-1401, 1997.

12. P. Dular, R. V. Sabariego and L. Krähenbühl, "Magnetic Model Refinement via a Perturbation Finite Element Method - From 1-D to 3-D," COMPEL, vol. 28, no. 4, pp. 974-988, 2009.

13. P. Dular and R. V. Sabariego, "A perturbation method for computing field distortions due to conductive regions with h-conform magnetodynamic finite element formulations," IEEE Trans. Magn., vol. 43, no. 4, pp. 1293-1296, 2007.

14. C. Geuzaine, B. Meys, F. Henrotte, P. Dular and W. Legros, "A Galerkin projection method for mixed finite elements," IEEE Trans. Magn., Vol. 35, No. 3, pp. 1438-1441, 1999.